Physics of the Solid State, Vol. 42, No. 1, 2000, pp. 96–102. Translated from Fizika Tverdogo Tela, Vol. 42, No. 1, 2000, pp. 93–99.

MAGNETISM AND FERROELECTRICITY

Antiferromagnetic Resonance in CuB_2O_4 Single Crystal

A. I. Pankrats, G. A. Petrakovskiĭ, and N. V. Volkov

Kirenskii Institute of Physics, Siberian Division, Russian Academy of Sciences, Akademgorodok, Krasnoyarsk, 660036 Russia
e-mail: pank@cc.krascience.rssi.ru

Received May 18, 1999

Abstract—The frequency–field, temperature, and angular dependences of the antiferromagnetic resonance parameters for the tetragonal CuB_2O_4 single crystal are studied in the frequency range 2.6–80 GHz and at temperatures of 4.2–30 K. The results obtained confirm the fact that, in the high-temperature state in the range 10–21 K, this compound is an easy-plane weak ferromagnet. The temperature dependence of the Dzyaloshinski field is determined. An abrupt change observed in the frequency–field dependence of the magnetic resonance at $T = 4.2$ K and $\mathbf{H} \perp C_4$ indicates the transition to the weak ferromagnetic state induced by the external field $H_\perp$. The phase diagram for CuB_2O_4 is constructed on the $H_\perp$–T coordinates. It is demonstrated that, in the low-temperature state, the magnetic moments of copper ions remain in the basal plane, but the weak ferromagnetism is absent. © *2000 MAIK "Nauka/Interperiodica".*

The discovery of the high-temperature superconductivity gave impetus to active research in copper oxide compounds. These materials possess a broad spectrum of magnetic structures from usual three-dimensional antiferromagnets (Bi_2CuO_4 [1]) to quasi-low-dimensional magnets with a spin-Peierls state ($CuGeO_3$ [2]) and a ladder structure ($KCuCl_3$ and $LiCu_2O_2$ [3, 4]).

Tetragonal CuB_2O_4 single crystals with the space group D_{2d}^{12} have been grown in recent experiments [5]. Preliminary studies [5–7] showed that, at temperatures below $T_N = 21$ K, this crystal is an easy-plane weak ferromagnet. According to the data on static magnetic measurements and heat capacity, the magnetic phase transition is observed at $T \approx 10$ K. It was assumed that this transition is the Morine transition from the weak ferromagnetic state to the collinear state with the easy anisotropy axis parallel to the C_4 axis [6, 7].

The aim of the present work was to investigate the frequency–field and temperature dependences of the magnetic resonance absorption in the CuB_2O_4 crystal in order to obtain additional information regarding the magnetic structure of this crystal, specifically in the low-temperature state.

EXPERIMENTAL

Samples of CuB_2O_4 were grown by the spontaneous crystallization technique [5].

The magnetic resonance measurements in the frequency range 28–80 GHz were carried out with a pulsed-magnetic-field spectrometer, in which the sample was placed in a plunged waveguide unit. In the frequency range 2.5–10 GHz, the measurements were performed on a magnetic resonance spectrometer with a stationary magnetic field: at a frequency of 2.5–6 GHz, the sample was mounted in a plunged coaxial unit, and, at 8–10 GHz, it was placed in a plunged waveguide or a resonant cavity.

RESULTS

Figures 1 and 2 depict the frequency–field dependences of the antiferromagnetic resonance in CuB_2O_4 at $T = 4.2$ K for two orientations of magnetic field with respect to the C_4 axis of the crystal: $\mathbf{H} \parallel C_4$ and $\mathbf{H} \perp C_4$. At $\mathbf{H} \parallel C_4$, the frequency–field dependence of the antiferromagnetic resonance is almost linear and tends to $\omega_c \approx 1.5$ GHz at $H \longrightarrow 0$. At $\mathbf{H} \perp C_4$, the frequency–field dependence also exhibits a small gap at $\omega_c = 2.4$ GHz (Fig. 2, inset 1). Moreover, an increase in the field leads to an abrupt change in the magnetic resonance frequency at $H \approx 12$ kOe. This portion of the frequency–field dependence of the antiferromagnetic resonance is displayed in inset 2 (Fig. 2).

The temperature dependences of the resonance parameters were measured at several frequencies for orientations of the external magnetic field along the C_4 axis and in the basal plane. Figure 3 shows the temperature dependences of the resonance field and the absorption linewidth at two frequencies and $\mathbf{H} \parallel C_4$. At both frequencies, the resonance field drastically decrease at $T \approx 8.5$ K, which is accompanied by a strong broadening of the absorption line. Upon further heating of the sample, the resonance field smoothly increases up to the value characteristic of the paramagnetic state at $T > 20$ K [6].

Figure 4 demonstrates typical temperature dependences of the resonance field measured at three different frequencies for the orientation $\mathbf{H} \perp C_4$. At frequencies of 10.6 and 28.65 GHz, the resonance field under-

goes a sharp change in the low-temperature range. The temperature that corresponds to this change in the resonance field decreases with an increase in the frequency. At a frequency of 56.59 GHz, the low-temperature anomaly of the resonance field is not observed down to $T = 4.2$ K. Upon heating, as the sample temperature approaches $T_N = 20$ K, the resonance field increases up to the value characteristic of the paramagnetic state. Moreover, the temperature range, in which the resonance field undergoes the above change, becomes narrower with a decrease in the frequency.

The temperature dependences of the linewidth at different frequencies for the orientation $\mathbf{H} \perp C_4$ are also shown in Fig. 4. It worth nothing that, at a frequency of 56.59 GHz, the linewidth, like the resonance field, does not exhibit anomalous behavior in the low-temperature range, whereas a pronounced broadening of the absorption line is observed at frequencies below ~45 GHz. As regards the broadening of the absorption line in the vicinity of T_N, the temperature range, in which this broadening takes place, becomes broader with an increase in the frequency of the experiment.

The angular dependences of the resonance field and the absorption linewidth for the magnetic field measured in the basal plane of the crystal for two frequencies at $T = 4.2$ K are displayed in Fig. 5.

DISCUSSION

In [6, 7], it was assumed that the tetragonal CuB_2O_4 crystal in the temperature range 10–21 K is an easy-plane weak ferromagnet with the spontaneous magnetic moment lying in the basal plane of the crystal. The energy density of this magnet can be written in the form [8]

$$F = J\mathbf{M}_1\mathbf{M}_2 - \mathbf{D}[\mathbf{M}_1 \times \mathbf{M}_2] - \mathbf{H}(\mathbf{M}_1 + \mathbf{M}_2) - K_1/2(\cos^2\beta_1 + \cos^2\beta_2) - K_2/2(\cos^4\beta_1 + \cos^4\beta_2). \quad (1)$$

Here, J is the exchange interaction constant; $\mathbf{M}_i$ are the magnetic moments of the sublattices; $\mathbf{D}$ is the Dzyaloshinski vector directed, in our case, along the $\mathbf{z} \parallel C_4$; K_1 and K_2 are the first-order and second-order constants of uniaxial anisotropy, respectively; and β_i are the angles between the magnetic moments of the sublattices and the principal crystal axis. The effective exchange field, Dzyaloshinski interaction, and uniaxial anisotropy field that correspond to relationship (1) are defined as follows:

$$H_E = JM_0, \quad H_D = DM_0, \quad H_{k1} = K_1/M_0,$$
$$H_{k2} = K_2/M_0,$$
$$M_0 = |\mathbf{M}_1| = |\mathbf{M}_2|.$$

If the transition observed in CuB_2O_4 at $T = 10$ K in weak fields is a spin-reorientation transition to the collinear antiferromagnetic state, it is caused by the change in sign of the effective uniaxial anisotropy field $H_a = H_{k1} + H_{k2}$. A similar transition referred to as the Morine transition is observed in hematite α-Fe_2O_3 at $T_M = 262$ K [8]. Below this temperature, the hematite transforms into the collinear antiferromagnetic state with the magnetic moments oriented along the principal crystal axis.

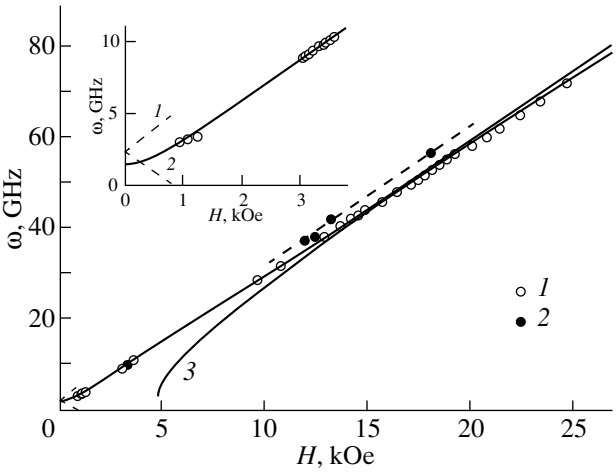

Fig. 1. Frequency–field dependences of the antiferromagnetic resonance in CuB_2O_4 for $\mathbf{H} \parallel C_4$ at $T =$ (*1*) 4.2 and (*2*) 13 K. The solid line corresponds to the results of calculations by formula (11). Dashed lines *1*, *2*, and *3* represent the data calculated by formulas (9) and (10) for ω_{21}, ω_{11}, and ω_{12}, respectively.

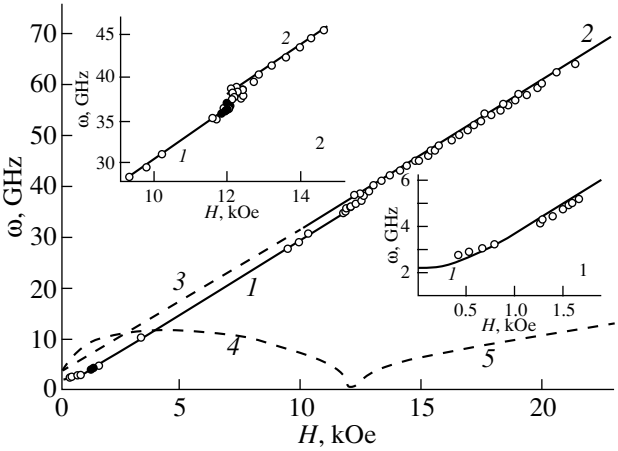

Fig. 2. Frequency–field dependences of the antiferromagnetic resonance in CuB_2O_4 for $\mathbf{H} \perp C_4$ at $T = 4.2$ K. Solid lines *1* and *2* correspond to the results of calculations for ω_{22} by formulas (7) and (5), respectively. Dashed lines *3*, *4*, and *5* represent the data calculated by formulas (4) and (5) for ω_{21}, ω_{11}, and ω_{12}, respectively.

Although the weak ferromagnetism is absent in the low-temperature collinear state, the Dzyaloshinski interaction affects the behavior of the antiferromagnet in the magnetic field [8–10]. Specifically, upon magne-

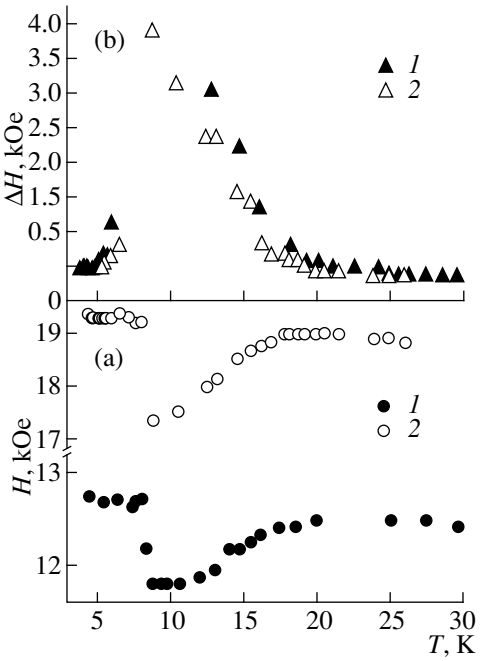

Fig. 3. Temperature dependences of (a) the resonance field and (b) the absorption linewidth for $\mathbf{H} \parallel C_4$. Frequency, GHz: (*1*) 37.76 and (*2*) 56.00.

tization along the principal crystal axis, the transition to the spin-flop state occurs in the critical field

$$H_c^2 = 2H_E(H_{k1} + H_{k2}) - H_D^2. \quad (2)$$

Upon magnetization in the basal plane of the crystal, the Dzyaloshinski interaction leads not only to the alignment of magnetic moments with the magnetic field, but also to the rotation of the antiferromagnetic vector $\mathbf{l} = (\mathbf{M}_1 - \mathbf{M}_2)/2M_0$ away from the principal crystal axis toward the basal plane. The angle θ between the C_4 axis and vector $\mathbf{l}$ increases with an increase in the magnetic field and reaches $\pi/2$ at the critical field $H_{c\perp}$

$$H_{c\perp} = (2H_E H_{k1} - H_D^2)/H_D. \quad (3)$$

In this case, depending on the ratio between the values of H_E, H_{k1}, H_{k2}, and H_D, the transition to the magnetic-field-induced weak ferromagnetic state at $H = H_{c\perp}$ can be eithera first-order or second-order phase transition.

As follows from the investigation on the temperature–field dependences of the magnetization for CuB_2O_4 [11], the critical field $H_{c\perp}$ depends on the temperature and reaches 12 kOe at $T = 4.2$ K. Upon magnetization along the C_4 axis at $T = 4.2$ K, the field dependence of the magnetization shows a weakly pronounced anomaly in the field $H = 2$ kOe, which can be taken as the critical field $H_{c\parallel}$. Using these values of the critical fields and the value of $H_D = 1.9$ kOe obtained in [6] for $T = 10$ K and also ignoring the temperature dependence of H_D below 10 K, at $T = 4.2$ K, we can calculate the parameters $2H_E H_{k1} = 26.41$ kOe^2 and $2H_E H_{k2} = -18.8$ kOe^2.

The resonance properties of an easy-axis antiferromagnet with the Dzyaloshinski interaction were discussed in detail in [8–10] on the condition that $H_a \ll H_D \ll H_E$, which holds true for CuB_2O_4. Let us use the results of these calculations to analyze the experimental data on the magnetic resonance in CuB_2O_4.

First and foremost, we consider the frequency–field dependences of the antiferromagnetic resonance measured at $T = 4.2$ K. It should be mentioned that the frequency jump at $\mathbf{H} \perp C_4$ occurs in the field coinciding with $H_{c\perp}$. For $\mathbf{H} \perp C_4$, the resonance frequencies at $H < H_{c\perp}$ (state 1) take the form

$$(\omega_{11}/\gamma)^2 = ((\omega_c/\gamma)^2 - 12H_E H_{k2}\sin^2\theta)\cos^2\theta,$$

$$(\omega_{21}/\gamma)^2 = (\omega_c/\gamma)^2 - 4H_E H_{k2}\sin^2\theta + H^2,$$

$$\sin\theta = HH_D/(2H_E(H_{k1} + 2H_{k2}\cos^2\theta) - H_D^2), \quad (4)$$

where $(\omega_c/\gamma)^2 = 2H_E(H_{k1} + 2H_{k2}) - H_D^2 = H_{c\parallel}^2 + 2H_E H_{k2}$ is the energy gap in the spectrum. In ω_{ij}, the subscript i is the number of vibrational mode, and the subscript j is the number of state.

In the field range $H > H_{c\perp}$ (state 2), the resonance frequencies are given by

$$(\omega_{12}/\gamma)^2 = HH_D - (2H_E H_{k1} - H_D^2) = H_D(H - H_E), \quad (5)$$

$$(\omega_{22}/\gamma)^2 = H(H + H_D).$$

The experimental data for $H > H_{c\perp}$ are adequately described by formula (5) for the high-frequency vibrational mode ω_{22}. The solid line in Fig. 2 represents the theoretical dependence at $H_D = 1.91$ kOe. At the same time, the resonance lines that correspond to the low-frequency vibrational mode ω_{12} (shown by the dashed line in Fig. 2) are not observed at the fields up to 80 kOe.

In the field range $H < H_{c\perp}$ (state 1), the experimental data coincide with none of the modes, which are described by expressions (4) and calculated with the above parameters $2H_E H_{k1}$ and $2H_E H_{k2}$. Furthermore, the ω_{11} and ω_{12} frequencies have real values beginning with the fields $H \approx 1$ kOe, whereas the energy gap ω_c and the frequencies of both vibrational modes in the fields $H < 1$ kOe are imaginary, which indicates that the ground state is chosen incorrectly.

Such a disagreement between the calculated and experimental data for the fields $H < H_{c\perp}$ and also the imaginary resonance frequencies could be explained by the fact that an incorrect experimental value of $H_{c\parallel}$ was used to determine the $2H_E H_{k2}$ parameter.

Hence, it is reasonable to describe the experimental data on the antiferromagnetic resonance by using for-

mulas (4) under the assumption that the $H_{c\perp}$ value and, therefore, the parameter $2H_EH_{k1}$ = 26.41 kOe^2 are uniquely determined from the experiment, and the $2H_EH_{k2}$ parameter can be obtained from the experimental energy gap ω_c = 2.4 GHz. This approach leads to $2H_EH_{k2}$ = –11.07 kOe^2. In this case, the theoretical frequency–field dependences (4) for ω_{11} and ω_{21} (shown by dashed lines in Fig. 2) are real over the entire range of fields from 0 to $H_{c\perp}$, but none of these curves coincides with the experimental frequency–field dependence.

Note that, at these values of $2H_EH_{k1}$ and $2H_EH_{k2}$, the calculated critical field $H_{c\|}$ is equal to 3.4 kOe; however, at this field, no specific features are observed in the experimental field dependence of the magnetization [11].

Another aspect is noteworthy. In [10], it was shown that, as the field increases from 0 to $H = H_{c\perp}$, the θ angle either continuously increases from 0 to $\pi/2$ (the second-order transition) or, first, continuously increases from 0 to $\theta_1 < \pi/2$ and, then, at the field $H = H_{c\perp}$, undergoes an abrupt change to $\theta = \pi/2$ (the first-order transition). The relationship for the ω_{21} frequency in the vicinity of $H = H_{c\perp}$ can be rewritten as follows:

$$(\omega_{21}/\gamma)^2 = H(H + H_D/\sin\theta). \qquad (6)$$

Consequently, upon transition from the collinear state to the weak ferromagnetic state, the change $\omega_{21} \longrightarrow \omega_{22}$ proceeds continuously for the second-order transition and in a stepwise fashion for the first-order transition, so that $\Delta\omega = \omega_{22} - \omega_{21} < 0$.

However, as is seen from Fig. 2, in our case, $\Delta\omega > 0$. Moreover, the experimental frequency–field dependence at T = 4.2 K in the field range from 0 to $H_{c\perp}$ is well described by the law

$$(\omega/\gamma_\perp)^2 = H^2(1 + |H_a|/2H_E) + H_\Delta^2 \qquad (7)$$

with $|H_a|/2H_E$ = 0.031 ± 0.005 and H_Δ^2 = (0.526 ± 0.004) kOe^2 (solid line in Fig. 2). Here, H_a is the effective field of anisotropy with respect to the C_4 axis, and H_Δ^2 is the isotropic energy gap, which can arise from magnetoelastic [12] or other interactions. The gyromagnetic ratio $\gamma_\perp$ = 2.983 MHz/Oe corresponds to the value $g_\perp$ = 2.133 obtained from the ESR experiment at room temperature [6]. Dependence (7) is characteristic of easy-plane antiferromagnets without weak ferromagnetism (see, for example, [13, 14]).

Therefore, the above findings put in doubt the fact that, as the temperature decreases, the weak ferromagnet CuB_2O_4 at T = 10 K transforms into the collinear state with the easy anisotropy axis aligned parallel to the C_4 axis.

It can be assumed that, in CuB_2O_4, the magnetic moments at T < 10 K also remain in the basal plane; however, the magnetic structure in this state allows no macroscopic spontaneous magnetic moment. Possible variants of this magnetic structure will be considered below.

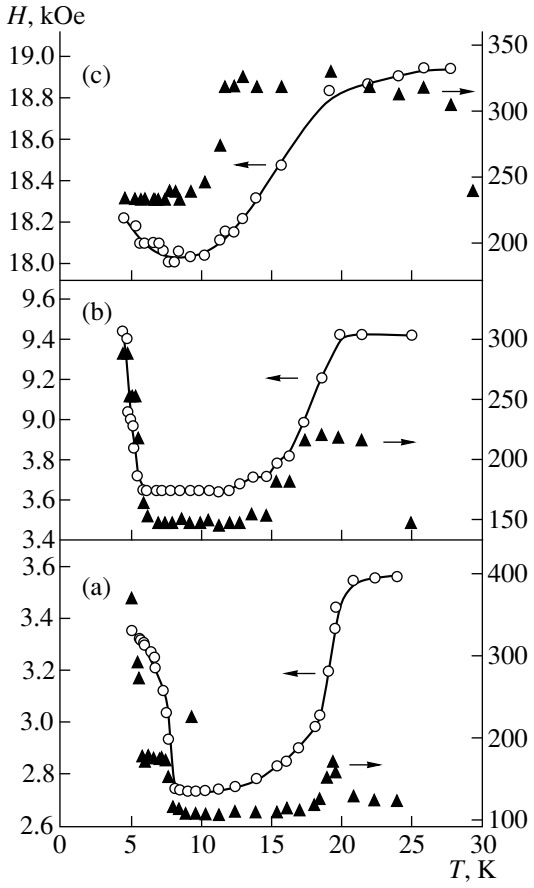

Fig. 4. Temperature dependences of the resonance field and the absorption linewidth for $\mathbf{H} \perp C_4$. Frequency, GHz: (a) 10.6, (b) 28.655, and (c) 56.59.

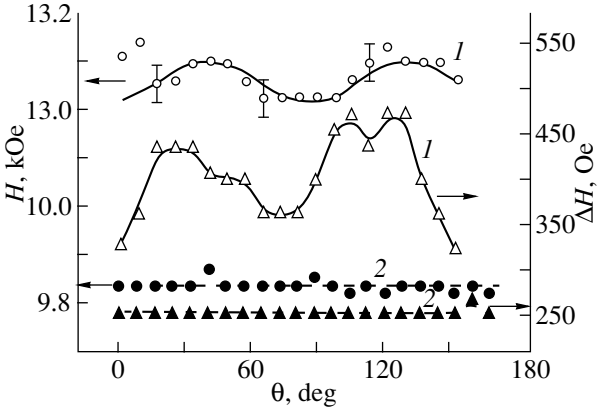

Fig. 5. Angular dependences of the resonance field and the absorption linewidth for $\mathbf{H} \perp C_4$. Frequency, GHz: (*1*) 41.51 and (*2*) 29.008.

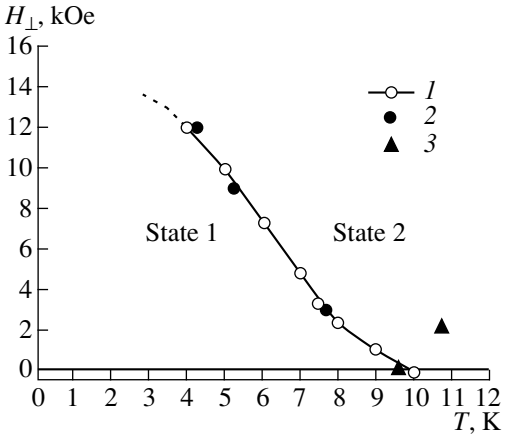

Fig. 6. The $H_\perp$–T phase diagram for CuB_2O_4 according to the data on (*1*) static magnetic measurements, (*2*) magnetic resonance, and (*3*) heat capacity.

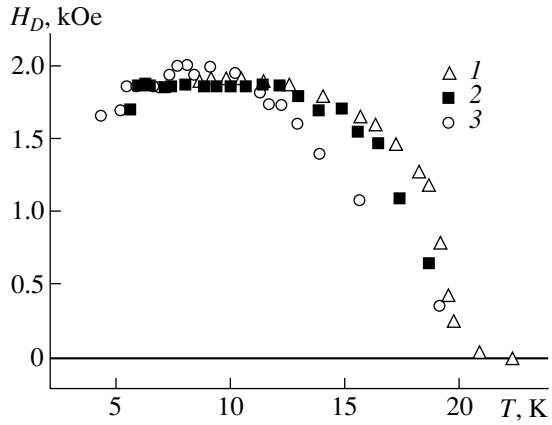

Fig. 7. Temperature dependences of the Dzyaloshinski field. Frequency, GHz: (*1*) 10.6, (*2*) 28.655, and (*3*) 56.59.

Sharply defined anomalies in the temperature dependences of the resonance parameters for CuB_2O_4 at $T < 10$ K (Fig. 4) are observed at some frequencies in the basal-plane fields. They are associated with the transition from the low-temperature state 1 to the weak ferromagnetic state 2 in the field $H_{c\perp}$. It is seen from Fig. 4 that the transition temperature depends on the frequency of the measurement, which suggests the temperature dependence of the critical field $H_{c\perp}$. Figure 6 demonstrates the $H_\perp$–T phase diagram constructed from the data on static magnetic measurements [11], heat capacity [7], and magnetic resonance. From the phase diagram, it is evident that the absence of low-temperature anomaly at a frequency of 56.09 GHz (Fig. 4c) is explained by the fact that, in the resonance field for this frequency (~18 kOe), the CuB_2O_4 crystal already at $T = 4.2$ K is in the magnetic-field-induced weak ferromagnetic state.

With equation (5) for ω_{22} and the temperature dependence of the resonance field for the weak ferromagnetic state, we calculated the temperature dependences of the Dzyaloshinski field $H_D(T)$ (Fig. 7). It is seen that thus obtained values of H_D are independent of the frequency of the measurement at temperatures below ~12 K. Above this temperature, as the temperature approaches T_N, the higher the frequency of a measurement, the steeper the dependence $H_D(T)$ declines to zero. This is likely due to the fact that the resonance fields corresponding to high frequencies of the measurement become comparable to the exchange field, which is anomalously weak in the CuB_2O_4 crystal [11]. As a result, the canting angle of magnetic sublattices φ in the external field cannot be treated as small, and, instead of equation (5), ω_{22} should be calculated by the formula [15]

$$(\omega_{22}/\gamma)^2 = H(H + |H_a|\sin\varphi + H_D\cos\varphi). \qquad (8)$$

It is clear that the role of this factor increases with a decrease in the H_E field as the temperature approaches T_N. Assuming that measurements at a frequency of 10.6 GHz give the $H_D(T)$ dependence, which is the closest to actual, and ignoring the contribution of H_a ($|H_a| \ll H_D, H$), we obtain that, in the resonance field $H \approx 18$ kOe corresponding to a frequency of 56.09 GHz, the canting angle of sublattices φ is equal to approximately 50° at $T = 15$ K.

The broadening of the absorption line in the vicinity of T_N at a frequency of 10.6 GHz is typical of the fluctuation broadening. Usually, an increase in the frequency of the measurement leads to a narrowing of the peak in the temperature dependence of the linewidth and a decrease in its height, because the strong field more efficiently suppresses fluctuations disturbing the magnetic ordering (see, for example, [16]). However, the reverse situation is observed for the CuB_2O_4 crystal: the peak in the temperature dependence of the linewidth is substantially broadened with an increase in the frequency. Moreover, at the same frequency, as the temperature approaches T_N, a clear correlation is observed between sharp broadening of the absorption line and the deviation from the true temperature dependence of the Dzyaloshinski field. Therefore, it is quite possible that such an unusual behavior of the linewidth is caused by the "collapse" of sublattices.

Let us now analyze the data on the magnetic resonance for the orientation $\mathbf{H} \parallel C_4$. In the case of a collinear antiferromagnet with the easy anisotropy axis aligned parallel to C_4, the frequency–field dependences have the form

$$\omega_{11,21}/\gamma = \omega_c/\gamma \pm H, \quad H < H_{c\parallel} \qquad (9)$$

$$(\omega_{12}/\gamma)^2 = H^2 - (2H_E H_{k1} - H_D^2), \quad H > H_{c\parallel} \qquad (10)$$

$$\omega_{22} = 0,$$

where ω_c/γ is the energy gap in the spectrum in the same form as in formula (4). The frequency–field dependences were calculated with the same values of $2H_EH_{k1}$ and $2H_EH_{k2}$ as in the case when $\mathbf{H} \perp C_4$. The calculated dependences of ω_{11}, ω_{21}, and ω_{12} (see Fig. 1 and inset) disagree with the experimental data. Furthermore, it follows from the calculations that, at the values used for $2H_EH_{k1}$ and $2H_EH_{k2}$, the resonance absorption should be absent at all in the field range from approximately 0.8 to 4.8 kOe; nonetheless, this absorption is observed experimentally.

Furthermore, the experimental frequency–field dependence of the antiferromagnetic resonance at T = 4.2 K for $\mathbf{H} \parallel C_4$ is smooth over the entire field range from 0.8 to 25 kOe and does not exhibit features accompanying the spin-reorientation transition from the easy-axis state to the spin-flop state. The absence of this transition at T = 4.2 K is also evidenced by anomalies in the temperature dependences of the resonance field and the linewidth (Fig. 3). Obviously, it is this abrupt change in the resonance field and this broadening of the absorption linewidth that are connected with the transition from the low-temperature state to the easy-plane weak ferromagnetic phase. Within the limits of experimental error, the temperature of the anomalies coincides with the transition temperature found from the heat capacity data [7] and does not depend on the external field, as would be the case of the transition from the easy-axis state to the easy-plane state.

At T = 4.2 K, the frequency–field dependence for $\mathbf{H} \parallel C_4$ is well represented by the relationship

$$(\omega/\gamma_\parallel)^2 = H^2 + H_\Delta^2 \qquad (11)$$

with $\gamma_\parallel = 2.92 \pm 0.01$ and $H_\Delta^2 = 0.26 \pm 0.03$ kOe^2 (solid line in Fig. 1). This dependence is characteristic of easy-plane antiferromagnets; in this case, the energy gap $H_\Delta^2 = 2H_EH_{k1} + H_D^2$. Certainly, a small value of the gap is surprising. However, the frequency–field dependence similar in character to relation (11) with the same value of H_Δ^2 is retained upon transition to the weak ferromagnetic state. An abrupt change in the resonance field upon this transition can be formally described by the variation in the g value from $g_\parallel = 2.087$ at T = 4.2 K to $g_\parallel = 2.210$ at T = 13 K. The reason for this behavior of the g value upon transition remains unclear.

Therefore, the resonance data for $\mathbf{H} \parallel C_4$ also indicate that CuB_2O_4 in the low-temperature phase is not collinear antiferromagnet with the easy anisotropy axis aligned parallel to the C_4 axis.

As regards the hypothetical magnetic structures, which could be realized in the low-temperature phase of CuB_2O_4, a possible cause of the absence of weak ferromagnetic moment in the low-temperature state resides in the fact that the adjacent, local weak ferromagnetic moments in this state are ordered antiferromagnetically. In particular, a similar structure is observed in the Y_2CuO_4 compound [17] and in the $YFe_{1-x}Cr_xO_3$ system [18]. These magnetic structures can be regarded as slightly noncollinear four-sublattice structures, which were investigated, for example, in [19]. Note that the external field applied across the basal plane of the Y_2CuO_4 crystal, as for the CuB_2O_4 crystal, induces the transition to the weak ferromagnetic state.

The absence of weak ferromagnetic moment in the low-temperature state of CuB_2O_4 can also be associated with a helical magnetic structure. A similar pattern is observed for the hexagonal $NiBr_2$ crystal [20]. In this crystal, the collinear magnetic ordering with the easy anisotropy plane perpendicular to the hexagonal axis is achieved at T_N = 52 K, and, with a further decrease in the temperature below T = 22.8 K, $NiBr_2$ transforms into the helical incommensurable phase. At temperatures below 22.8 K, the external magnetic field applied across the basal plane destroys the helical structure and transforms this crystal to the easy-plane collinear state.

The occurrence of the helical magnetic structure in the low-temperature state of CuB_2O_4 can be supported by the presence and absence of the angular dependence of the resonance parameters in the basal plane at fields above and below $H_{c\perp}$, respectively. In the absence of external magnetic field, the local antiferromagnetic vectors in the helical structure are uniformly distributed over all directions in the basal plane. Under the external magnetic field, the helicoid is distorted and transformed into a fanlike structure, in which the antiferromagnetic vectors are distributed within the sector of angular size α. If the α value is comparable to the period of tetragonal angular dependence ($\pi/2$), the averaging over all the local positions results in the absence of the angular dependence of the resonance parameters in the basal plane.

For the refinement of the magnetic structure of CuB_2O_4, it is necessary to perform the neutron diffraction analysis of this crystal.

Thus, in the present work, we studied the frequency–field and temperature dependences of the resonance absorption in the tetragonal CuB_2O_4 single crystal.

At T = 4.2 K, the frequency–field dependence at $\mathbf{H} \perp C_4$ exhibits an abrupt change in the field $H \approx$ 12 kOe, which is connected with the transition from the low-temperature state to the weak ferromagnetic state. It is found that the temperature of this transition depends on the magnetic field $H_\perp$ applied across the basal plane of the crystal and is independent of the field along the C_4 axis.

The phase diagram for the CuB_2O_4 crystal is constructed on the $H_\perp$–T coordinates.

In the weak ferromagnetic state, the frequency–field dependence at $\mathbf{H} \perp C_4$ is typical of easy-plane antifer-

romagnets with the Dzyaloshinski interaction. The temperature dependence of the Dzyaloshinski field is determined from the experimental data at temperatures of 4.2–20 K.

An analysis of the frequency–field dependences at $T = 4.2$ K demonstrates that CuB_2O_4 in the low-temperature phase is not a collinear antiferromagnet with the easy anisotropy axis aligned parallel to the C_4 axis. It is assumed that, upon transition to the low-temperature state, the magnetic moments remain in the basal plane of the crystal, but the resulting magnetic structure allows no weak ferromagnetic moment.

ACKNOWLEDGMENTS

We would like to thank K.A. Sablina for the growth of high-quality CuB_2O_4 single-crystals and A.M. Vorotynov for fruitful discussions.

This work was supported by the Krasnoyarsk Regional Scientific Foundation, project no. 8F0156.

REFERENCES

1. G. A. Petrakovskiĭ, K. A. Sablina, A. I. Pankrats, *et al.*, J. Magn. Magn. Mater. **140–144**, 1991 (1995).
2. G. A. Petrakovskiĭ, Izv. Vyssh. Uchebn. Zaved., Fiz. (1), 91 (1998).
3. H. Tanaka, K. Takatsu, W. Shiramura, *et al.*, J. Phys. Soc. Jpn. **65** (7), 1945 (1996).
4. A. M. Vorotynov, A. I. Pankrats, G. A. Petrakovskiĭ, *et al.*, Zh. Éksp. Teor. Fiz. **113** (5), 1866 (1998).
5. G. A. Petrakovskiĭ, K. A. Sablina, D. A. Velikanov, *et al.*, Kristallografiya, 1999 (in press).
6. G. A. Petrakovskiĭ, K. A. Sablina, D. A. Velikanov, *et al.*, Fiz. Tverd. Tela (St. Petersburg) **41** (7–8) (1999).
7. G. Petrakovskiĭ, D. Velikanov, A. Vorotinov, *et al.*, J. Magn. Magn. Mater., 1999 (in press).
8. I. S. Jacobs, R. A. Beyerlein, S. Foner, *et al.*, Int. J. Magn. **1** (1), 193 (1971).
9. V. I. Ozhegin and V. G. Shapiro, Zh. Éksp. Teor. Fiz. **54** (1), 96 (1968).
10. V. I. Ozhegin and V. G. Shapiro, Zh. Éksp. Teor. Fiz. **55** (5), 1737 (1968).
11. G. A. Petrakovskiĭ, A. D. Balaev, and A. M. Vorotynov, Fiz. Tverd. Tela (St. Petersburg, 1999) (in press).
12. A. S. Borovik-Romanov and E. G. Rudashevsky, Zh. Eksp. Teor. Fiz. **47** (6), 2095 (1964).
13. A. I. Pankrats, D. Yu. Sobyanin, A. M. Vorotinov, *et al.*, Solid State Commun. **109** (4), 263 (1999).
14. L. P. Regnault, J. Rossat-Mignod, A. Adam, *et al.*, J. Phys. (Paris) **43** (8), 1283 (1982).
15. A. G. Gurevich, *Magnetic Resonance in Ferrites and Antiferromagnets* (Nauka, Moscow, 1973).
16. E. G. Rudashevsky, V. N. Seleznyov, and L. V. Velikov, Solid State Phys. **11** (8), 959 (1972).
17. A. Rouco, X. Obradors, M. Tovar, *et al.*, Phys. Rev. B: Condens. Matter **50** (14), 9924 (1994).
18. A. M. Kadomtseva, A. S. Moskvin, I. G. Bostrem, *et al.*, Fiz. Tverd. Tela (Leningrad) **19** (6), 2286 (1977).
19. E. A. Turov, *Physical Properties of Magnetically Ordered Crystals* (Akad. Nauk SSSR, Moscow, 1963).
20. A. Adam, D. Billerey, C. Terrier, *et al.*, Phys. Lett. A **79** (4), 353 (1980).

Translated by O. Borovik-Romanova